Supplementary Information

A Fundamental Flaw in Current Construction of TiO_2 Electron Transport Layer of Perovskite Solar Cells and Its Elimination

Yan Yan[#1, 3, 4], Cheng Liu[#2], Yi Yang[2], Guoxiang Hu[5], Vandana Tiwari[4, 7], De-en Jiang[6], Wei Peng[1], Ajay Jha[4, 11, 12], Hong-Guang Duan[4, 8, 9], Friedjof Tellkamp[4], Yong Ding[2], Weidong Shi[3], Shouqi Yuan[3], Dwayne Miller[4, 9,], Wanhong Ma[1, 10]*, Jincai Zhao[1, 10]

1 Beijing National Laboratory for Molecular Sciences, Key Laboratory of Photochemistry, CAS Research/Education Center for Excellence in Molecular Sciences, Institute of Chemistry, The Chinese Academy of Sciences, Beijing 100190, China

2 State Key Laboratory of Alternate Electrical Power System with Renewable Energy Sources, North China Electric Power University, Beijing 102206, China

3 School of Chemistry and Chemical Engineering, Jiangsu University, No. 301, Xuefu Road, Zhenjiang, 212013 China

4 The Max Planck Institute for the Structure and Dynamics of Matter, Luruper Chaussee 149, 22761 Hamburg, Germany

5 Department of Chemistry and Biochemistry，Queens College of the City University of New York，Queens，New York 11367，United States

6 Department of Chemistry, University of California, Riverside, California 92521, US

7 Department of Chemistry, University of Hamburg, Martin-Luther-King Platz 6, 20146 Hamburg, Germany

8 Institut für Theoretische Physik, Universitat Hamburg, Jungiusstraße 9, 20355 Hamburg, Germany

9 The Departments of Chemistry and Physics, University of Toronto, 80 St. George Street, Toronto, Canada

10 University of Chinese Academy of Sciences, Beijing 100049, China

11 The Rosalind Franklin Institute, Harwell Campus, Didcot, Oxfordshire OX11 0FA, UK

12 Research Complex at Harwell, Rutherford Appleton Laboratory, Didcot OX11 0QX, UK

[#] **Author contribution:** authors contribute equally to this paper.

[*]**Corresponding author. Email:**

whma@iccas.ac.cn (W. Ma)

Supplementary Methods

Chemicals

Lead (II) iodide (99.99%, trace metals basis) was purchased from TCI (Japan), and CH_3NH_3I was purchased from Xi'an Polymer Light Technology Corp. (China). TiO_2 pastes (18-nm and 30-nm, anatase) were obtained from Dyesol (Australia). Sodium hydroxide (NaOH) and sodium ethoxide (EtONa) were purchased from Acros (Beijing, China). DMF, chlorobenzene, lithium bis (trifluoromethylsulfonyl) imide (Li-TFSI) and 4-tert-butylpyridine (tBP) were purchased from Aldrich (U.S.), and spiro-MeOTAD was acquired from Xi'an Polymer Light Technology (China). All of the above reagents were used as received.

Homemade 15-nm TiO_2 nanocrystal paste was prepared according to reference (*1*) by using 15-nm anatase TiO_2 powder purchased from Alfa (Shanghai, China). In a typical preparation procedure, 1 g of TiO_2 nanoparticles, 4.06 g of terpineol and 5 mL of ethanol were mixed under vigorous agitation. Then, 4.5 mL of a solution of ethylcellulose in ethanol was added to the mixture. The resulting solution was further stirred and sonicated for 24 h. The excess ethanol was then removed from the solution using a rotary evaporator at 58°C to obtain a viscous paste. The concentrated paste was redissolved in ethanol to 15 $_{wt}$% before use.

Preparation of normal TiO_2 ETLs

A thick, dense blocking layer of TiO_2 (bl-TiO_2) was first deposited onto an F-doped SnO_2 (FTO) substrate by spin coating to prevent direct contact between the FTO and the hole-conducting layer. The precursor solution contained 0.6 mL of titanium isopropoxide and 0.4 mL of bis(acetylacetonate) in 7 mL of anhydrous isopropanol. The resulting TiO_2 blocking layer was then sintered at 460°C. A mesoporous TiO_2 layer (mp-TiO_2) with a thickness of approximately 160-180 nm was then deposited by spin coating onto the bl-TiO_2/FTO substrate. A 15 $_{wt}$% ethanol paste of anatase TiO_2 nanocrystals was used as the mp-TiO_2 precursor. After spin coating, the substrate was immediately dried on a hotplate at 120°C and then calcined at 460°C~550°C to remove the organic components. Unless stated otherwise, the normal TiO_2 ETLs were all prepared at 550°C.

Preparation of NaOH-TiO_2 and EtONa-TiO_2 ETLs

Similar to the preparation of normal TiO_2 ETLs, a thick, dense bl-TiO_2 layer was first deposited onto the FTO substrate by spin coating. An mp-TiO_2 layer was then deposited onto the bl-TiO_2/FTO substrate. Before coating the mp-TiO_2 layer, 0.1 mL of ethanolic NaOH or EtONa at specific concentrations was first added to 1 mL of mp-TiO_2 precursor (15 wt% ethanol paste) to create a basic paste. The mass ratios of the added base to TiO_2 were 0.34 wt%~1.36 wt% for NaOH and 0.67 wt%~2.68 wt% for EtONa. Then, the basic paste was used as the precursor of the deprotonated mp-TiO_2 layer. After spin coating, the substrate was immediately dried on a hotplate at 120°C and then calcined at 460°C~550°C to remove the organic components. Unless otherwise stated, all NaOH-TiO_2 and EtONa-TiO_2 ETLs were prepared at 550°C.

Preparation of the H^+-TiO_2 ETLs

Similar to the preparation of normal TiO_2 ETLs, a thick, dense bl-TiO_2 layer was first deposited onto the FTO substrate by spin coating. An mp-TiO_2 layer was then deposited onto the bl-TiO_2/FTO substrate. Before coating the mp-TiO_2 layer, 0.1 mL of an aqueous solution at pH=1~10 (adjusted with H_2SO_4 or NaOH) was added to 1 mL of mp-TiO_2 precursor solution to load various amounts of protons into the TiO_2 nanocrystals. After spin coating, the substrate was immediately dried on a hotplate at 120°C and then calcined at 550°C to remove the organic components.

Preparation of Na_2SO_4-TiO_2, NaCl-TiO_2 and KCl-TiO_2 ETLs

Similar to the preparation of normal TiO_2 ETLs, a thick, dense bl-TiO_2 layer was first deposited onto the FTO substrate by spin coating. An mp-TiO_2 layer was then deposited onto the bl-TiO_2/FTO substrate. Before coating the mp-TiO_2 layer, 0.1 mL of aqueous solution of Na_2SO_4 (1.40 wt% to TiO_2), NaCl (1.15 wt% to TiO_2) or KCl (1.46 wt% to TiO_2) was first added to 1 mL of mp-TiO_2 precursor (15 $_{wt}$% ethanol paste). After spin coating, the substrate was immediately dried on a hotplate at 120°C and then calcined at 500°C to remove the organic components.

Quantification of the residual protons in the TiO_2 ETLs

The proton content in TiO_2 ETLs was quantified by a back titration using NaOH solution and the MAS-NMR ^{1}H spectra. We used the H^+-TiO_2 ETL (pH =1) sample as the typical reference sample, and it was first titrated with aqueous NaOH. In a typical titration procedure, the H^+-TiO_2 ETL sample was removed from its FTO substrate and ground into a fine powder. Then, 100 mg of H^+-TiO_2 powder was immersed in 5 mL of 0.05 M NaOH aqueous solution and allowed to stand for 30 min. After separation by centrifugation, the H^+-TiO_2 ETL sample for titration was washed several times. The resulting supernatant was collected and then diluted to 25 mL. Standard aqueous HCl solution (25 mL, 0.01 M) was then employed to back titrate the residual NaOH in the supernatant to calculate the amount of NaOH consumed to determine the titratable acidic protons on the H^+-TiO_2 ETL (pH =1) sample. After titration with 0.05 M aqueous NaOH, an $MAPbI_3$ layer was coated on the titrated H^+-TiO_2 ETL powder (using CH_3NH_3I and PbI_2 in DMSO and DMF (v/v=1:4) as mentioned above) as an internal reference to compare the decrease in the intensity of the acidic proton signal in the MAS-NMR ^{1}H spectrum of the resulting $MAPbI_3$/TiO_2 sample, as shown in **Fig. S2**. This change can be used to calculate the total proton content. Under our experimental conditions, the acidic protons in the H^+-TiO_2 ETL (pH =1) that titrated with 0.05 M NaOH was 2.6×10^{-7} mol/mg TiO_2. According to the decrease in the relative intensity of the 6.35 ppm peak (assigned to the acidic protons) after titration, the total acidic protons in the H^+-TiO_2 ETL (pH =1) sample as calculated to be 1.24×10^{-6} mol/mg TiO_2. Accordingly, the proton content in all the other samples can be calculated according to the intensity of their 6.35 ppm peak relative to their 3.31 ppm peak (assigned to C-H in $MAPbI_3$) in their MAS-NMR ^{1}H spectrum, as shown in **Table S1**.

Computational method.

DFT calculations were performed using the Vienna *ab initio* simulation package (VASP) (*2*). The electron exchange correlation was represented by the functional of Perdew, Burke, and Ernzerhof of generalized gradient approximation (*3*). The ion–electron interactions were described with the projector augmented-wave method (4). The convergence threshold for structural optimization was set to 0.025 eV/Å in force. The climbing-image nudged elastic band method implemented in VASP was used to determine the energy barrier (5). The transition states were obtained by relaxing the force below 0.05 eV/Å. For the hydrogen adsorption calculations, the TiO_2/$MAPbI_3$ interface was modeled by the (101)-TiO_2/(110)-$MAPbI_3$ surface with a low interface lattice mismatch (6). A 3×5×3 perovskite slab containing 45 $MAPbI_3$ units combined with a 5×3×2 anatase TiO_2 slab containing 120 TiO_2 units was used. A vacuum of 15 Å along the z-direction was employed. To save computational time, a smaller system (3×3×2 perovskite slab and 5×2×2 anatase TiO_2 slab) was used for the energy barrier calculations.

The average hydrogen adsorption energies (ΔE_H values) at the perovskite/TiO_2 interface were calculated by $\Delta E_H = [E(\text{interface} + 30H) - E(\text{interface}) - 15E(H_2)]/15$, where E(interface + 30H) and E(interface) represent the total energies of the perovskite/TiO_2 interface with thirty adsorbed hydrogens and zero adsorbed hydrogens, respectively. $E(H_2)$ represents the total energy of one H_2 molecule in the gas phase. A negative value of ΔE_H suggests favorable adsorption.

References

(1) Y. Kusumawati, M. A. Martoprawiro, Th. Pauporté, *J. Phys. Chem. C* **118**, 9974-9981 (2014)

(2) G. Kresse, J. Furthmüller, *Phys. Rev. B*: *Condens. Matter Mater. Phys.* **54**, 11169–11186 (1996)

(3) J. Perdew, K. Burke, M. Ernzerhof, *Phys. Rev. Lett.*, **77**, 3865– 3868 (1996)

(4) P. Blöchl, *Phys. Rev. B: Condens. Matter Mater. Phys.* **50**, 17953– 17979 (1994).

(5) G. Henkelman, B. Uberuaga, H. Jónsson, *J. Chem. Phys.* **113**, 9901– 9904 (2000).

(6) E. Mosconi, E. Ronca, F. De Angelis, *J. Phys. Chem. Lett.* **5**, 2619–2625 (2014).

Supplementary Figures and Tables:

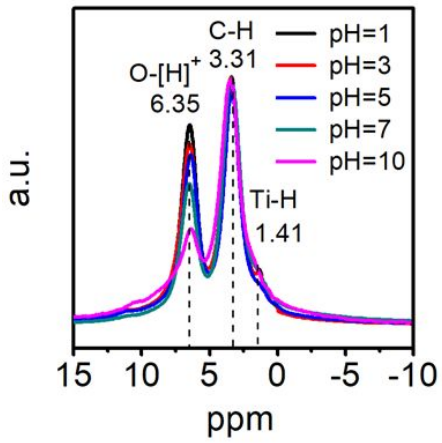

Fig. S1. MAS-NMR ^{1}H spectra of $MAPbI_3/TiO_2$ samples with H^+-TiO_2 ETLs prepared by adding aqueous solutions with pH=1~10 (adjusted with H_2SO_4 or NaOH) into the paste.

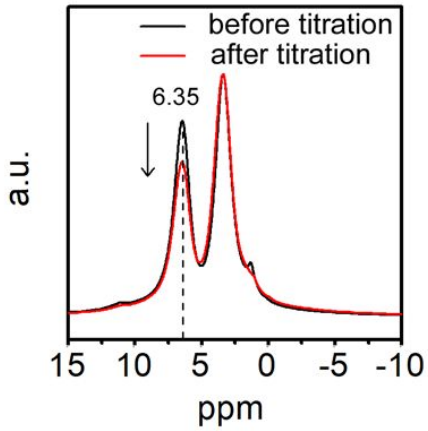

Fig. S2. MAS-NMR ^{1}H spectra of $MAPbI_3/TiO_2$ samples with H^+-TiO_2 ETL (pH=1) before and after titration with 0.05 M aqueous NaOH.

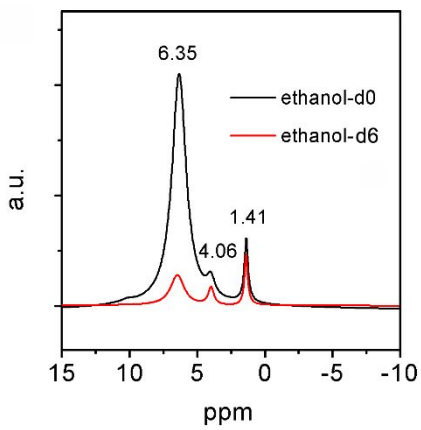

Fig. S3. The MAS ^{1}H NMR spectra of the normal TiO_2 samples prepared by using ethanol-d_0/d_6 as the solvent in the precursor paste.

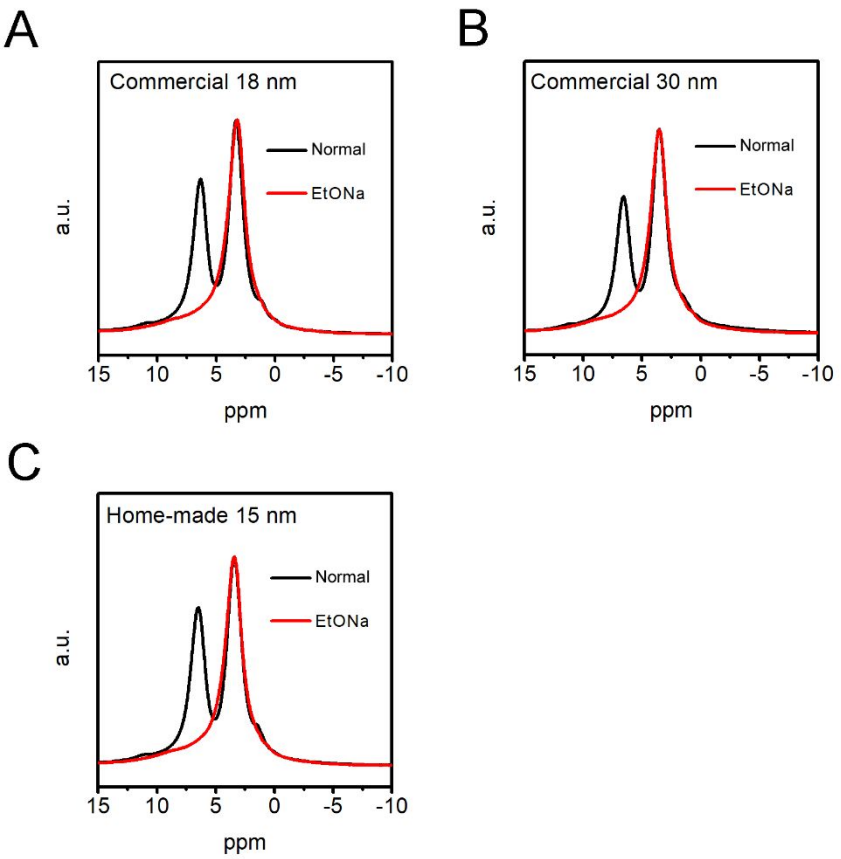

Fig. S4. (A) The MAS ^{1}H NMR spectra of the $MAPbI_3/TiO_2$ samples with normal and EtONa-TiO_2-1.34 ETLs prepared with **(A)** commercial 18-nm TiO_2 paste, **(B)** commercial 30-nm TiO_2 paste and **(C)** homemade 15-nm TiO_2 paste. All the TiO_2 pastes were in the anatase phase.

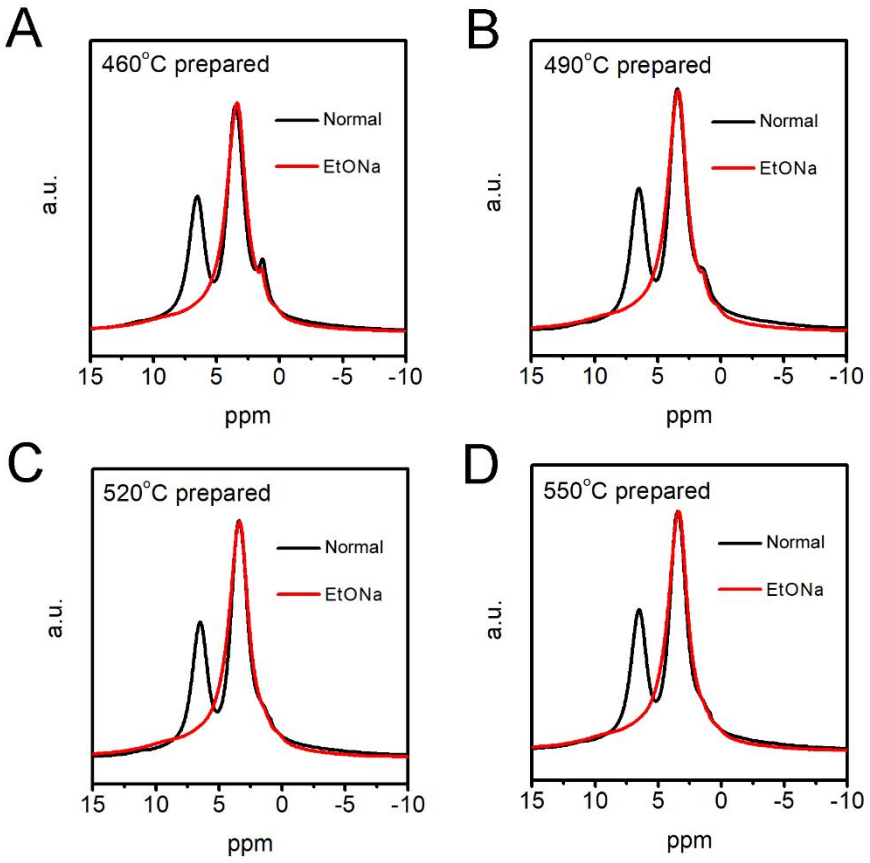

Fig. S5. MAS ^{1}H NMR spectra of $MAPbI_3/TiO_2$ samples with normal and EtONa-TiO_2-1.34 ETLs prepared at **(A)** 460°C, **(B)** 490°C, **(C)** 520°C and **(D)** 550°C.

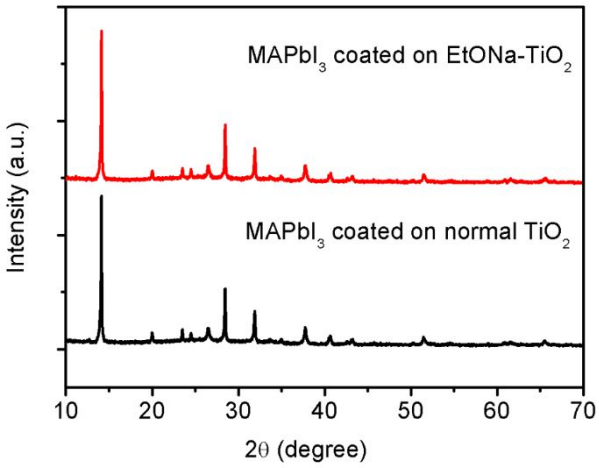

Fig. S6. XRD spectra of $MAPbI_3$ layer that coated on the normal TiO_2 ETL and EtONa-TiO_2-1.34 ETL.

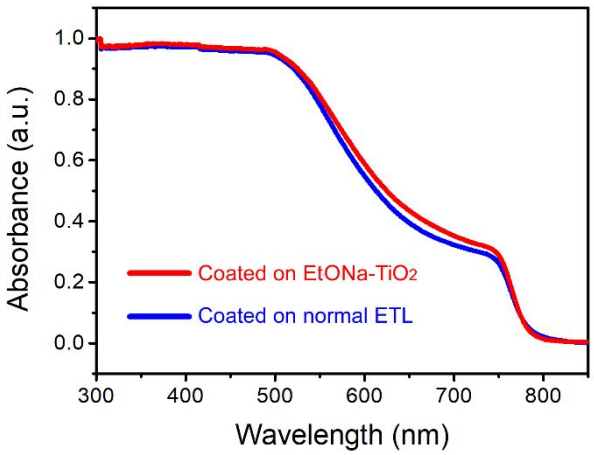

Fig. S7. UV-vis absorption spectra of $MAPbI_3$ perovskite layers coated on normal and EtONa-TiO_2-1.34 ETLs.

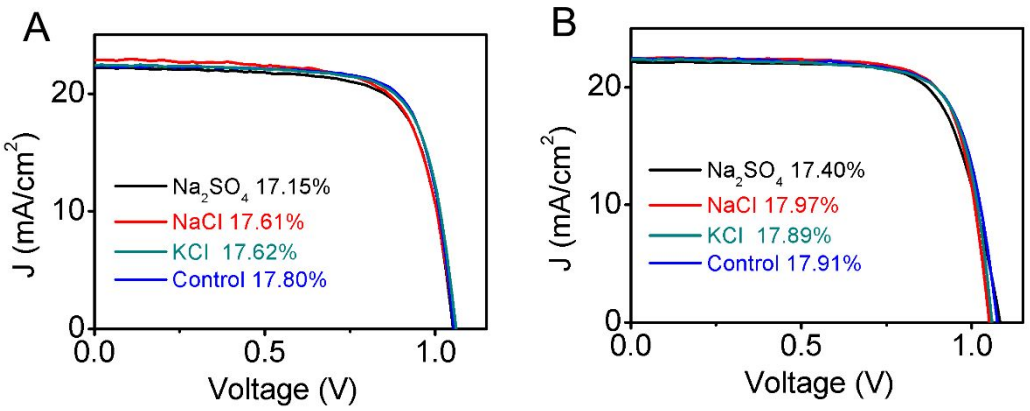

Fig. S8. *J-V* characteristics determined under simulated AM1.5 G illumination of $MAPbI_3$ **(A)** and $FA_{0.85}MA_{0.15}PbI_{2.55}Br_{0.45}$ **(B)** PSC devices with normal TiO_2 (control), Na_2SO_4-TiO_2, NaCl-TiO_2 and KCl-TiO_2 ETLs.

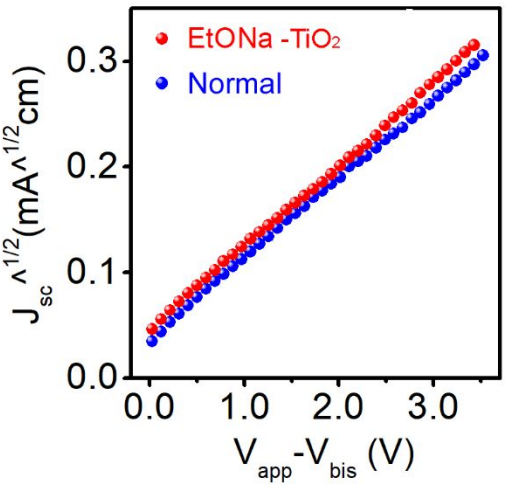

Fig. S9. Space-charge-limited current (SCLC) curves of FTO/TiO_2/Au devices with normal and EtONa-TiO_2-1.34 ETLs.

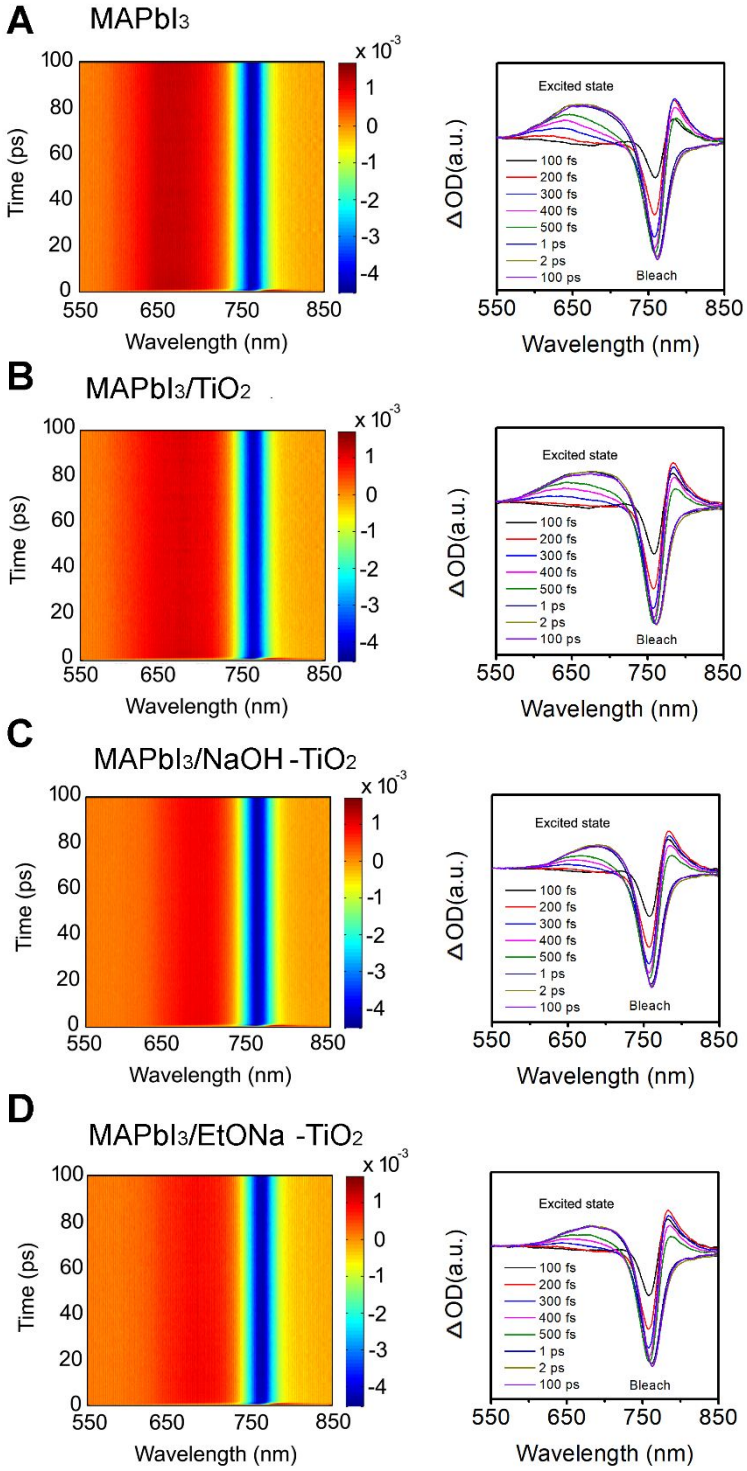

Fig. S10. Femtosecond transient absorption: 2D map (left) and spectral traces for selected time points (right) recorded following 515 nm laser pulse excitation of **(A)** pristine $MAPbI_3$, **(B)** $MAPbI_3/TiO_2$, **(C)** $MAPbI_3/NaOH\text{-}TiO_2$-0.34 and **(D)** $MAPbI_3/EtONa\text{-}TiO_2$-1.34 samples.

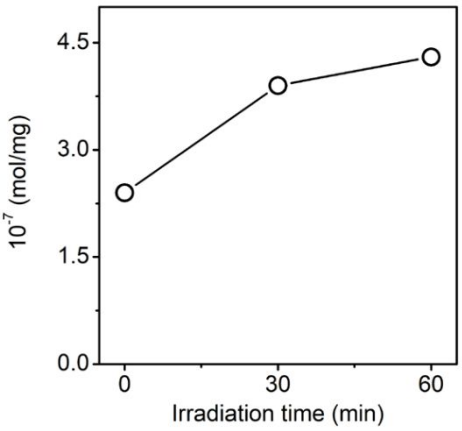

Fig. S11. The increase of Ti-H in 60 min irradiation on the $MAPbI_3/TiO_2$ sample with normal TiO_2 ETL. (The quantification based on the MAS-NMR peak intensity profiles in Table S2)

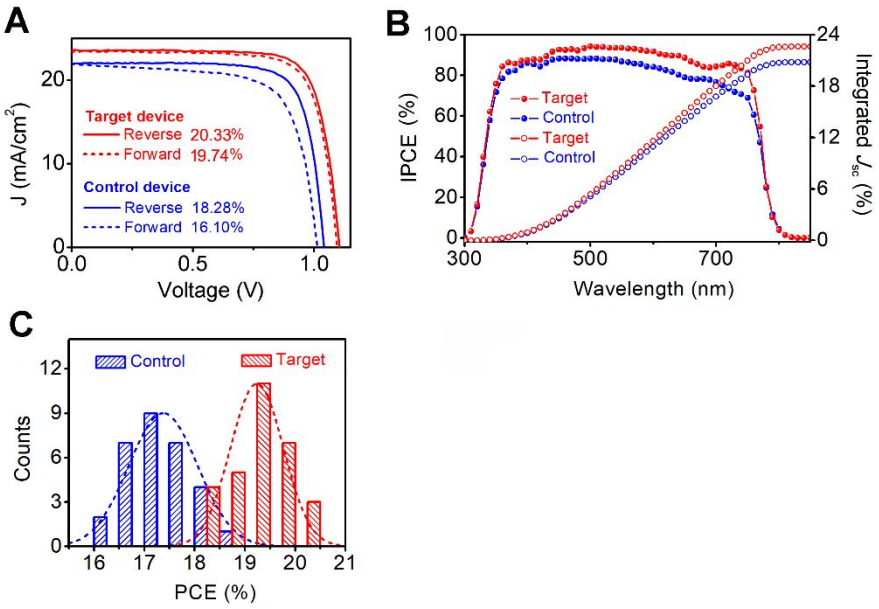

Fig. S12. (A) *J-V* characteristics of optimized devices with $MAPbI_3$ PSCs determined under simulated AM1.5 G illumination for the control (with a normal TiO_2 ETL) and target (with a EtONa-TiO_2-1.34 ETL) devices with reverse and forward scans. The details of the photovoltaic parameters are shown in Table S4. **(B)** The corresponding incident photon-to-current conversion efficiencies (IPCEs) and the integrated J_{sc} spectra of the control and target devices. **(C)** Histogram extracted from a comparison of PCEs of 30 batches (60 devices) of control and target devices.

Supplementary Tables

Table S1. Peak intensity profiles of MAS-NMR ^{1}H spectra of $MAPbI_3/TiO_2$ samples with different TiO_2 ETLs. (All peaks are normalized with the 3.31 ppm peak as 1)

Samples	6.35 ppm (H^+)	3.31 ppm (C-H)	1.41 ppm (Ti-H)	H^+ amount (mol/mg)
H^+-TiO_2 (H_2SO_4)	1.57	1.00	0.24	2.37×10^{-6}
H^+-TiO_2 (HCl)	1.06	1.00	0.16	1.60×10^{-6}
H^+-TiO_2 (HAc)	1.21	1.00	0.25	1.83×10^{-6}
H^+-TiO_2 (pH=1)	0.82	1.00	0.23	1.24×10^{-6}
H^+-TiO_2 (pH=3)	0.74	1.00	0.20	1.12×10^{-6}
H^+-TiO_2 (pH=5)	0.69	1.00	0.17	1.05×10^{-6}
H^+-TiO_2 (pH=7)	0.57	1.00	N/A	8.70×10^{-7}
H^+-TiO_2 (pH=10)	0.39	1.00	N/A	5.95×10^{-7}
Normal	0.72	1.00	0.17	1.11×10^{-6}
NaOH-TiO_2-0.34	N/A	1.00	N/A	N/A
EtONa-TiO_2-1.34	N/A	1.00	N/A	N/A

Table S2. Quantification of hydrogen terminals based on the peak intensity profiles of MAS-NMR ^{1}H spectra of $MAPbI_3/TiO_2$ samples under different irradiation time with normal TiO_2 ETLs. (All peaks are normalized with the 3.31 ppm peak as 1)

Samples	6.35 ppm (H^+)	3.31 ppm (C-H)	1.41 ppm (Ti-H)	H^+ amount (mol/mg)	Ti-H amount (mol/mg)
Normal TiO_2 (0 min)	0.724	1.00	0.16	1.09×10^{-6}	2.4×10^{-7}
Normal TiO_2 (30 min)	0.602	1.00	0.26	9.06×10^{-7}	3.9×10^{-7}
Normal TiO_2 (60 min)	0.587	1.00	0.30	8.83×10^{-7}	4.3×10^{-7}

Table S3. Photovoltaic parameters of the $MAPbI_3$ devices with Et-O-Na-TiO_2 ETLs prepared with different EtONa mass ratios (0.67 $_{wt}$%~2.68 $_{wt}$%) to TiO_2 in the basic paste.

EtONa content	V_{oc} (V)	J_{sc} (mA/cm^2)	FF (%)	PCE (%)
0 $_{wt}$%	1.03	22.52	75.63	17.55
0.67 $_{wt}$%	1.06	23.96	75.73	19.20
1.34 $_{wt}$%	1.10	23.50	77.68	20.11
2.01 $_{wt}$%	1.05	22.95	78.34	18.83
2.68 $_{wt}$%	1.03	23.66	75.59	18.46

Table S4. Photovoltaic parameters of the $MAPbI_3$ devices with NaOH-TiO_2 ETLs prepared with different NaOH mass ratios (0.34 $_{wt}$%~1.36 $_{wt}$%) to TiO_2 in the basic paste.

NaOH concentration	V_{oc} (V)	J_{sc} (mA/cm^2)	FF (%)	PCE (%)

0 $_{wt}$%	1.02	22.55	76.59	17.57
0.34 $_{wt}$%	1.03	23.84	77.62	19.11
0.68 $_{wt}$%	1.06	22.84	77.83	18.88
1.02 $_{wt}$%	1.04	22.61	77.50	18.28
1.36 $_{wt}$%	1.05	22.27	76.84	17.91

Table S5. Photovoltaic parameters of the optimized target and control $MAPbI_3$ devices with normal and EtONa-TiO_2-1.34 ETLs.

Devices	**Scan direction**	**V_{oc} (V)**	**J_{sc} (mA/cm^2)**	**FF (%)**	**PCE (%)**
Target device	Reverse	1.11	23.42	78.04	20.33
	Forward	1.10	23.56	76.92	19.74
Control device	Reverse	1.04	22.61	77.50	18.28
	Forward	1.02	22.51	70.38	16.10

Table S6. Photovoltaic parameters of the optimized target and control $FA_{0.85}MA_{0.15}PbI_{2.55}Br_{0.45}$ devices with normal and EtONa-TiO_2-1.34 ETLs.

Devices	**Scan direction**	**V_{oc} (V)**	**J_{sc} (mA/cm^2)**	**FF (%)**	**PCE (%)**
Target device	Reverse	1.13	23.51	79.03	21.00
	Forward	1.13	23.27	78.26	20.57
Control device	Reverse	1.07	22.42	74.33	17.91
	Forward	1.04	22.44	64.16	15.01